AIAA JOURNAL
Vol. 30, No. 10, October 1992

Time-Averaged, Three-Dimensional Flow in a Rectangular Sudden Expansion

Jean R. Hertzberg*
University of Colorado, Boulder, Colorado 80309
and
Chih Ming Ho†
University of California, Los Angeles, Los Angeles, California 90024

An experimental study of a 2:1 aspect ratio rectangular jet that undergoes a 6:1 sudden expansion in area is being conducted to understand the three-dimensional dynamics of the asymmetric vortex rings formed in the confined shear layers and thus to understand entrainment and mixing in this type of configuration. LDV is used to measure three velocity components under forced and unforced conditions. Profound differences are found between the two axes of symmetry: in contrast to a conventional two-dimensional sudden expansion, no time-averaged recirculation is found in the minor axis plane. Along the major axis a normal size recirculation zone is found. Significant transverse velocities are the result of both rapid spreading of the jet on the minor axis and the effects of confinement by the duct on the developing jet. In this paper the time-averaged flow pattern is described, and mass fluxes are compared at two streamwise locations. These results are presented not only to illustrate new flow phenomena but also to serve as a database. The phase-averaged properties and a discussion of the vortex dynamics will be presented in a companion paper that is under preparation.

Introduction

RECENT advances have been made in the control of mixing by the use of techniques that affect the behavior of the coherent structures formed in shear layers. These vortex structures are, in turn, responsible for the entrainment of fluid into the shear layer and thus are responsible for controlling the mixing process. Coherent structure control techniques have been demonstrated in jets using asymmetric nozzle shapes and in shear layers using periodic flow perturbations. One important application for these passive and active forcing techniques is in propulsive combustors, such as ramjets, where the control of mixing can be crucial both for increasing combustion efficiency and for the controlling of characteristic instabilities.

Passive control of mixing can be achieved through the use of asymmetric jets, i.e., not plane-symmetric or axisymmetric jets. For instance, small-aspect-ratio elliptic jets have been found to have entrainment ratios several times larger than either plane symmetric or axisymmetric jets.[1] This high entrainment has been attributed to the dynamics of the noncircular vortex rings that form as coherent structures in the jet shear layers. These dynamics are governed by self-induction, the effect of one portion of the vortex ring on another. This causes the regions of the vortex rings with higher curvature to convect ahead of the rest, which, in turn, increases the curvature of the lagging portions. These portions then overtake and decrease the curvature of the initial high curvature sections.[2] As a result, the elliptical shape is restored, but the axis that was initially the minor axis has become the major axis, and the motion then begins again. Up to seven cycles of axis switching have been observed in the evolution of isolated free elliptic vortex rings.[3] This behavior is also seen in the vortex rings formed in the shear layers of elliptic and rectangular jets and is responsible for the increased entrainment and axis switching observed.

Active forcing in the form of periodic flow perturbations has been found to be effective in controlling both free shear layers and flow over backward-facing steps by encouraging (or discouraging) pairing of the large-scale structures that are responsible for much of the entrainment.[4-7] Active forcing is also useful since it organizes the shear layer by reducing the phase jitter of the large structures and thus allows ensemble averaging based on the phase angle.

Application of these active and passive mixing control techniques to combustion systems is expected to increase combustion efficiency by causing faster spreading shear layers and thus increased mixing. Enhanced mixing between burned and unburned gases in premixed combustion systems can result in better flame stabilization and higher turbulent burning velocities. In non-premixed combustion systems, enhanced mixing can result in larger distributed reaction zones. Faster spreading shear layers are particularly important in dump combustors, since a shorter recirculation zone will allow a shorter overall design. These considerations led to the choice of a forced rectangular sudden expansion for study. Various similar configurations have been examined by Schadow et al.[5,8,9] and Gutmark et al.[10] both with and without combustion. Increased mixing and higher centerline temperatures were found, confirming the utility of these configurations.

An extensive survey of the flowfield in a suddenly expanded, low-aspect-ratio rectangular jet has been made to determine the effect of passive and active forcing on the recirculation zone structure in isothermal flow. The results presented here include time-averaged measurements of three velocity components in the major and minor axis planes from $x/h = 0.5$ to 5.0 and in cross sectional planes at $x/h = 0.5$ and 3.0.

Experimental Description

The experiments were carried out in a vertical water channel consisting of a 2:1 aspect ratio rectangular jet (7.62 × 3.81 cm) that underwent a sudden expansion with uniform step height h equal to the minor side length (Fig. 1). The flow was driven by a constant 3.6-m head system, and the flow rate was controlled at the exit. Screens were placed in the channel upstream of the expansion at $x/h = -1$, -2, and -3 to insure uniform flow and a thin initial boundary layer. The freestream turbulence intensity was 1.1%. Active forcing was provided by a

Received April 17, 1991; revision received Jan. 16, 1992; accepted for publication April 6, 1992.

*Assistant Professor, Department of Mechanical Engineering. Senior Member AIAA.

†Professor, Department of Mechanical, Aerospace and Nuclear Engineering. Senior Member AIAA.

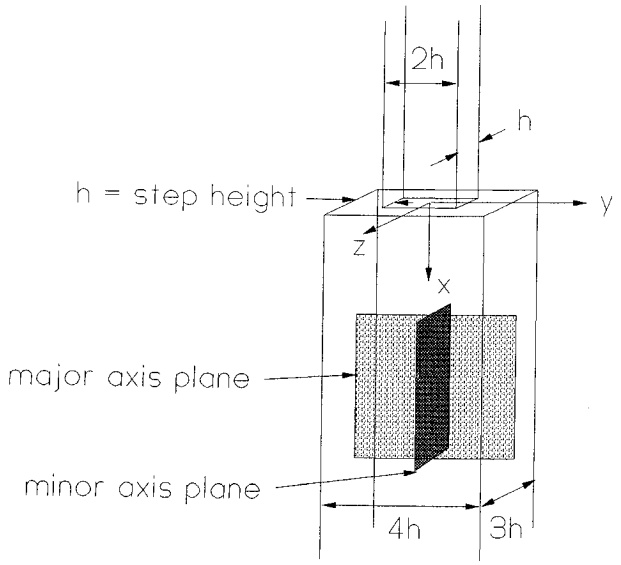

Fig. 1 The flow configuration: a rectangular sudden expansion.

global pressure perturbation, created by passing a small portion of the exit flow through a computer-controlled, rotating butterfly valve, resulting in an approximately sinusoidal fluctuation in the initial jet velocity. With the exception of the initial trials, the forcing level of the data reported here was 3% rms and the forcing was at 2 Hz. The Reynolds number was $Re_h = 8.5 \times 10^3$, where $Re_h = U_0 h/\nu$ and $U_0 = 21.6$ cm/s, the initial jet velocity measured at the centerline, $x/h = 0.5$. Coordinates are specified from the centerline of the jet in the plane of the expansion with x as the streamwise direction, y along the major axis, and z along the minor.

Quantitative velocity measurements of the flow under steady-state conditions were made with a two-component, frequency shifted laser Doppler velocimeter (LDV). A 0.4-W argon ion laser was used. The optics were the Dantec 55X three beam system, with expansion and a 310-mm lens, resulting in a measurement volume of 1.1 by 0.09 mm. Two TSI IFA-550 counters were used. The signals were converted to analog and then sampled at 100 Hz to avoid velocity bias effects. The individual counter data rates ranged from 5 kHz in the low-velocity regions to more than 20 kHz in the high-velocity regions. The analog outputs were sampled within 1μs of each other. Examination of the raw data revealed that the assumption of continuous data was reasonable under these conditions, even in regions of high turbulence. Bias effects are thus considered negligible.[11-13] The naturally occurring particulate matter in tap water, filtered to 5 μ, was used as seeding. All data acquisition and the optics traversing mechanism were controlled by an IBM AT compatible computer. Mean values and rms fluctuations were calculated at each measurement location from 32,000 samples.

Measurements were made in the major and minor axis half-planes, from 0.5 to 5.0 step heights downstream, on a grid with 0.1667 h spacing. Measurements were spaced more closely in the high shear regions, although measurements in the boundary layers were not made. Data were also taken in transverse planes at $x/h = 0.5$ and 3, with the aforementioned spacing. The U and V were measured simultaneously, as were U and W.

Despite the screens in the inlet section, the flow in the potential core at $x/h = 0.5$ was not a perfect "top hat." The inlet flow was measured on a 0.17h (6.35-mm) grid across the entire inlet area at $x/h = 0.5$. The maximum deviation from uniformity in the jet potential core was 5% of U_0, and the average of the deviations throughout the core was 0.24%. These deviations, although undesirable, were symmetric and repeatable. An analysis of the quadrant-to-quadrant variation in U throughout the inlet jet core was made. The differences between quadrants at any location in the core was less than 1.6% U_0. Data containing an inlet profile from $y/h = 0$ to 2 were taken on four separate occasions, over a six-month period. The rms of the differences between the four profiles was typically 0.5% U_0 at any location across the profile, with the exception of the center of the shear layer, where the rms was 6% U_0. Two of the four repeats were taken as direct traverses, where the data were acquired sequentially from the centerline out. The other two profiles are reassembled from the first measurement location of streamwise traverses. This demonstrates the day-to-day repeatability. Uncertainty in the measurements is due to statistical considerations, signal processing, and flow fluctuations. The total estimated uncertainty ranges from 0.5% U_0 at the centerline to 2% U_0 in the regions near the walls.

Results

Planes of Symmetry

Since the recirculation zone length is of primary importance to any application using a sudden expansion, the first quantitative measurements made were of the velocity near the walls (at a distance of 0.083h) in the symmetry planes. Previous studies of unconfined small-aspect-ratio elliptic jets found more rapid spreading in the minor axis plane. This led to the expectation that the recirculation zone would be shorter on the minor axis than on the major, since the step height on both axes was equal. Instead, scans of the streamwise velocity component U near the walls yielded no recirculation at all in the minor axis plane, as shown in Fig. 2. Recirculation was found in the major axis plane, which shows a recirculation zone length of approximately 10 step heights, which is slightly long for these conditions,[14,15] that is, a laminar shear layer (determined by flow visualization) that becomes turbulent before reattachment. However, this length is only estimated because both the location of zero velocity was beyond the range of the traverse, and the velocity was not measured at the wall surface. In addition, the presence of high turbulence in these regions and the low frequency unsteadiness characteristic of separated flows[16,17] contributed to an estimated uncertainty of 0.02 U_0. This estimate is based on repeated tests for convergence of the data near the end of the recirculation zone.

The effect of low level (1%) active forcing on these results was investigated next. Studies by Bhattacharjee[6] et al. and Roos and Kegelman[7] found active forcing to significantly affect the recirculation zone length in backward-facing step flows and attributed this effect to manipulation of the formation and pairing processes of large vortical structures in the shear layers. Figure 3 compares the positive (nonrecirculating)

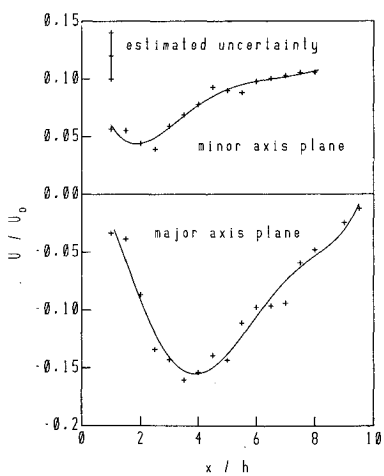

Fig. 2 Streamwise velocities in unforced flow, 0.083h from the side walls.

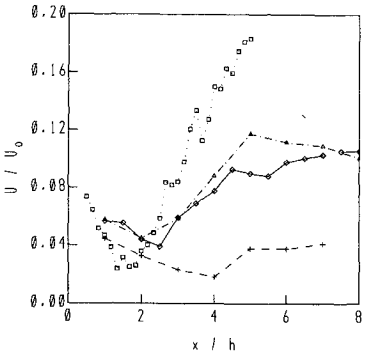

Fig. 3 Streamwise velocity near wall in minor axis plane at $y/h = 0$ and $z/h = 1.417$ for various forcing frequencies: ◇ and solid line = unforced; + and dashed line = 1% forcing at fundamental frequency; Δ and dash-dot = 1% forcing at first subharmonic; □ and dotted line = 1% forcing at second subharmonic.

flow along the wall in the minor axis plane at $z/h = 1.417$, $y/h = 0.0$, under various forcing frequencies. The dominant frequency in the unforced shear layer at $x/h = 0.5$ is referred to as the fundamental. This is the most amplified frequency of the initial free shear layer at $x/h = 0.5$ and is 8 Hz in the present study. Forcing at the fundamental frequency reduced the positive flow on the minor axis, possibly by inhibiting the vortex pairing process in the shear layer and thus reducing the spreading rate (Mode I in Ho and Huang[4]). In this case, the high-speed fluid from the jet does not penetrate to the wall region, and therefore the velocity near the wall is lower than in the unforced flow case. Forcing at the first subharmonic gave results close to the unforced case, and forcing at the second subharmonic increased the positive flow near the wall. This could be due to the encouragement of early pairing or the initial formation of larger vortices, which would result in more rapid spreading of the shear layer and thus higher positive velocities near the wall. This last case was chosen for further study because this frequency (2 Hz) also corresponds to the preferred mode of the jet column, i.e., the dominant frequency found at the end of the potential core in the unforced case. Forcing at this low frequency also allows the tracking of the large vortex structures farther downstream via the phase averaging technique. In addition, the interesting phenomenon, that is, the lack of recirculation on the minor axis, is more apparent for this forcing condition.

These unusual findings indicated that extensive flow mapping was required to understand the basic flow pattern in this configuration. The flow was determined to be reasonably symmetric across the major and minor axis planes. Although plane-symmetric sudden expansions are characterized by asymmetric recirculation zones,[18] axisymmetric sudden expansions are not.[19,20] A study of a square channel expansion by Nakao[21] found symmetry just after the expansion but asymmetry farther downstream. This asymmetry was attributed to construction details. Studies of wall-bounded rectangular jets by Holdeman and Foss[22] and Shimizu et al.[23] found three-dimensional symmetric flow and related the secondary flow development to vortex self-induction. In fact, Armaly et al.[24] found symmetric, three-dimensional flow behind a single backward-facing step of aspect ratio 1:36 for transitional Reynolds numbers such as that of the present study. The configuration of the present study could be considered a hybrid of the two extremes, plane-symmetric and axisymmetric expansions, and thus either the case of symmetry or asymmetry would not be unexpected. However, Cherdron et al.[18] attributed the marked asymmetry of the plane-symmetric expansion to antisymmetric interaction between vortexes in the two confined shear layers. In this study the symmetric nature of the active forcing would tend to suppress this mechanism, and thus the symmetry found was not surprising. Streamwise velocity data in the minor axis plane were symmetric across the centerline to within an average of 3.25% of U_0. In the transverse measurement plane at $x/h = 3$, quadrant-to-quadrant variations were within 6% of U_0. Detailed measurements of (U, V) were made in the $(+y, -z)$ quadrant, and measurements of (U, W) were made in the $(+y, +z)$ quadrant. The U is averaged from the two data sets unless otherwise noted, and the data are mirrored where appropriate.

Selected time-averaged velocity vectors in the major and minor axis planes are shown in Fig. 4. The mean velocity component perpendicular to those shown is negligible: there was no mean flow across the axes of symmetry. The upstream half of the recirculation zone is seen in the major axis plane, Fig. 4a, and the transverse velocity component V is significant only within the first two step heights downstream, where the recirculating flow is returned to positive flow. Further downstream, the velocity vectors are parallel, indicating little transverse flow. In contrast, the transverse flows in the minor axis plane, as seen in Fig. 4b, display considerable outward flow in the downstream portions as the jet spreads rapidly toward the walls. This is demonstrated by the diverging velocity vectors in the jet. The transverse flow into the jet close behind the step is similar to that of the major axis plane. Also note that there is no time-averaged recirculating flow anywhere in the minor axis plane, with the possible exception of the narrow region less than half a step height from the expansion, which was inaccessible to the LDV. In this region a small "secondary" zone may exist.

Figure 5 examines the axial velocity component in more detail. One half of the major axis plane is shown, and nonmirrored data of the full minor axis plane are presented to demonstrate the flow symmetry. The maximum recirculation velocity in the major axis plane is 19% of U_0 at $x/h = 3.0$, whereas in the minor axis plane the jet spread results in a positive flow of 8% of U_0 near the wall at $x/h = 3.0$ that increases to 18% at $x/h = 0.5$. Measurements were not made in the boundary layer; the measurement location closest to the wall was $0.083h$ from the surface. Figure 5 also shows the spreading of the shear layers. At $x/h = 0.5$, the shear layer thickness is $0.205h$ in the major axis, as determined by the steepest gradient method using $U/U_0 = 1$ and 0 as intercepts. This thickness is initially comparable to that of the minor axis, $0.202h$, and, in fact, the shear layer thicknesses remain comparable with downstream distance. However, the trajectories of the shear

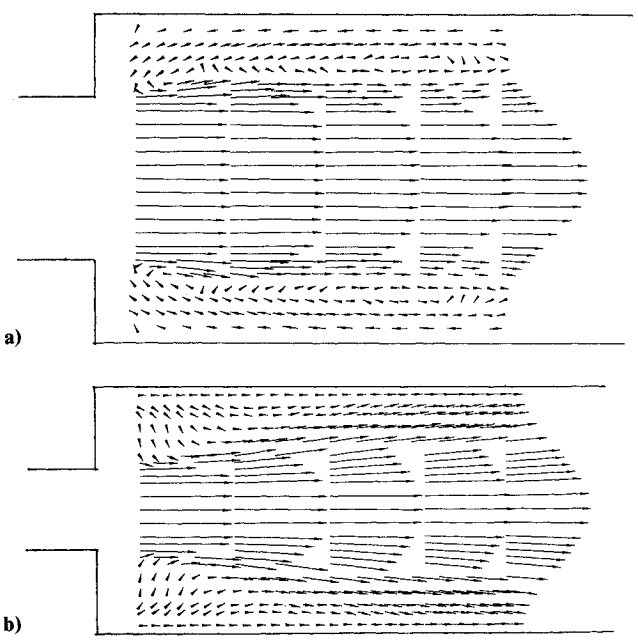

Fig. 4 Velocity vectors: a) major axis plane and b) minor axis plane.

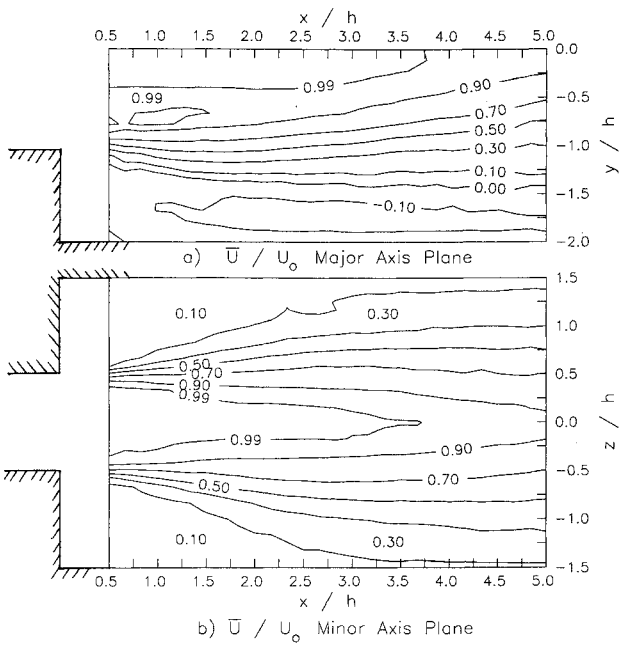

Fig. 5 Contours of $\bar{U}/U_0$ in the a) major axis plane and b) minor axis plane.

layers in the two planes differ significantly. In the major axis plane the shear layer originates at $y/h = 1$, and in the minor axis plane it originates at $z/h = 0.5$, whereas in both planes it is centered at $0.75h$ from the centerline by the end of the measurement region. Thus the layer has moved inward toward the centerline in the major axis plane and outward toward the wall in the minor axis plane.

The shear layer trajectories are also followed by the fluctuation intensity contours, Figs. 6 and 7. The streamwise fluctuations u' reach a peak in the shear layer near $x/h = 3.25$ in both the major and minor axes, coincident with the end of the potential core. The major axis peak, at 29% of U_0, is significantly higher than that of the minor axis, at 22%. In addition, u' in the minor axis has two peaks, a narrow one early in the shear layer and a broader peak three step heights downstream. By comparison, a brief review of maximum axial fluctuation intensities in axisymmetric expansions given in Morrison et al.[25] has a range of 18–30%. Bhattacharjee et al.[6] reported that low level active forcing could increase fluctuation intensities in a backward-facing step flow with turbulent separation by 50%. Roos and Kegelman[7] compared the increase in streamwise fluctuations for a forced backward facing step between laminar and turbulent initial shear layers ($Re_h = 9.5 \times 10^3$ and 3.9×10^4) and found the increase in fluctuations to be even more pronounced for the case of laminar separation. The maximum forced intensity reported by Bhattacharjee et al.[6] was 18% and that of Roos and Kegelman[7] was 24%. Schadow et al.[9] studied active forcing in an axisymmetric expansion and found increases of 30% due to forcing two diameters downstream. Their maximum at that location was 25%, found at the centerline, rather than in the shear layer.

The transverse velocity fluctuations, v' in the major axis and w' in the minor axis, reach peaks of 24 and 22% close to $x/h = 1.0$. These peaks are probably related to the rollup of the large vortex structures in the forced shear layer. That these peaks are somewhat lower than the axial fluctuations is consistent with other sudden expansion studies.[25-27] The velocity fluctuations perpendicular to the planes of symmetry, w' in the major axis plane and v' in the minor axis plane, are shown in Figs, 6c and 7b. These fluctuations are of the same order of magnitude as the streamwise and transverse fluctuations, although the mean flows perpendicular to the planes of symmetry are zero. The peaks occur halfway between the peaks in the streamwise and transverse peaks in each plane.

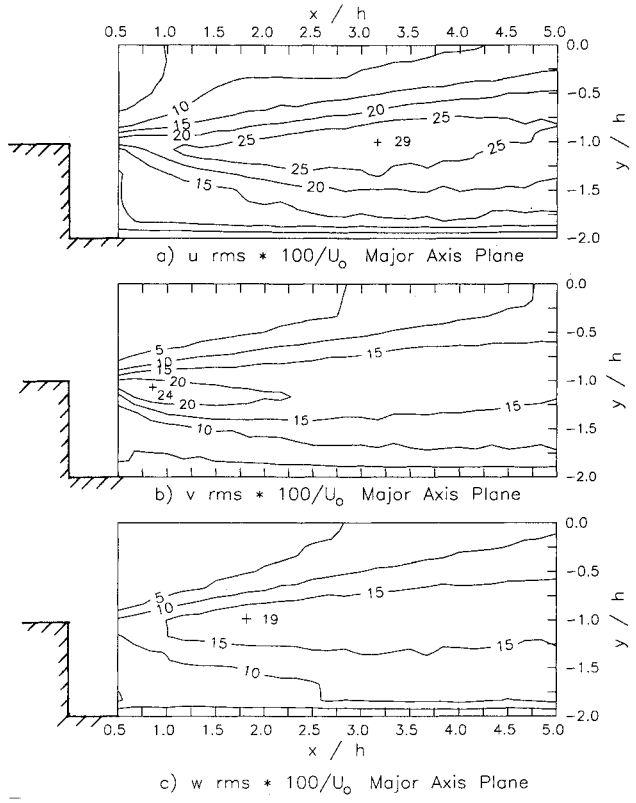

Fig. 6 Contours of velocity fluctuations in the major axis plane, percentage of U_0: a) u', b) v', and c) w'.

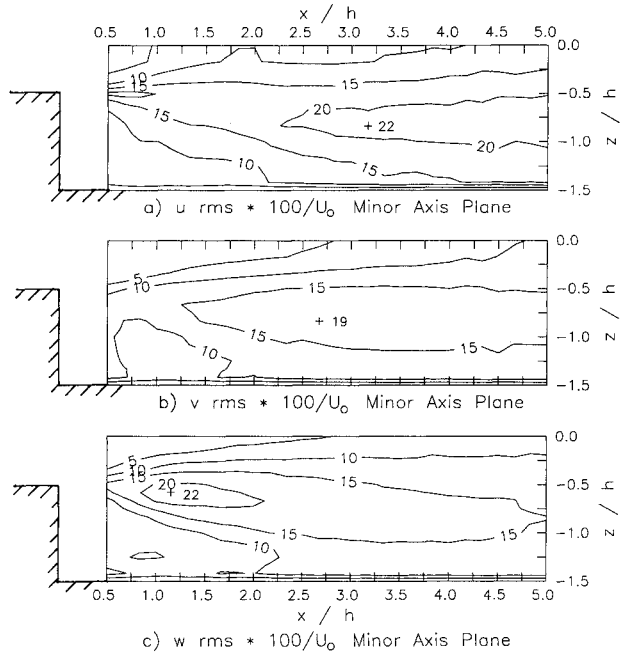

Fig. 7 Contours of velocity fluctuations in the minor axis plane, percentage of U_0: a) u', b) v', and c) w'.

Transverse Planes

Figures 8a and 8b show the velocity vectors projected into the transverse planes at $x/h = 0.5$ and 3.0, respectively. These will be referred to as the upper and lower measurement planes. The rectangle in the center represents the initial jet shape. In the upper plane in the potential core, both transverse velocity components V and W are nearly zero. Most noticeable is the strong V component found everywhere outside of the jet, with the exception of the region near the minor axis, where the flow is primarily inward toward the centerline. This results in a half

saddle point in this plane at the walls at the ends of the minor axis. The flow into the jet on the minor axis can be explained with reference to the free elliptic jet,[1] which showed higher entrainment on the minor axis. Thus, the minor axis region acts as a sink, pulling fluid inward. Because of the confinement, this fluid must come from the side regions, hence the V component.

At three step heights downstream of the expansion, the picture has changed dramatically, as shown in Fig. 8b. Here the flow is primarily in the W direction, outward away from the major axis. When this flow reaches the wall, it is apparently redirected into the outer corners of the expansion, where it again turns back toward the major axis. The circuit is not closed, however; the axial component U is needed in both planes to complete the picture and satisfy continuity.

The axial mean velocity at $x/h = 0.5$ is shown in Fig. 9. Since the steep gradients would make a contour plot difficult to interpret, these mirrored data are plotted in an orthographic surface representation. The jet core is rectangular at this upstream station. The flow surrounding the jet is slightly negative, with the exception of the flow near the minor axis, which is positive. When coupled with the transverse velocity information, this indicates that flow from the recirculation zone found on the major axis is feeding the positive flow on the minor axis.

In the lower measurement plane, Fig. 10, the recirculating flow is stronger and is seen to extend the width of the channel, (The hatchure marks point toward the local minimum.) The

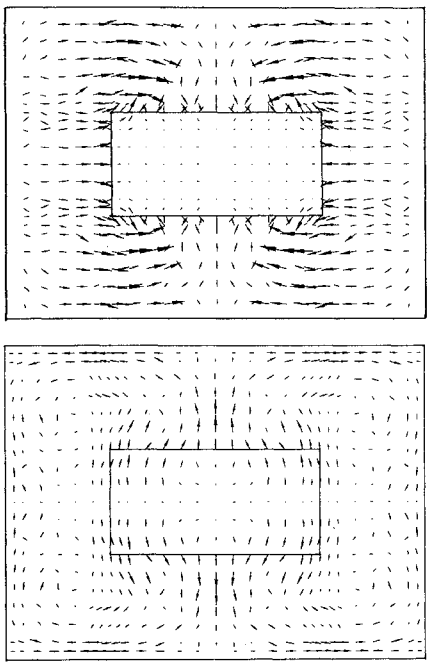

a)

b)

Fig. 8 Transverse velocity vectors at a) $x/h = 0.5$, and b) $x/h = 3.0$.

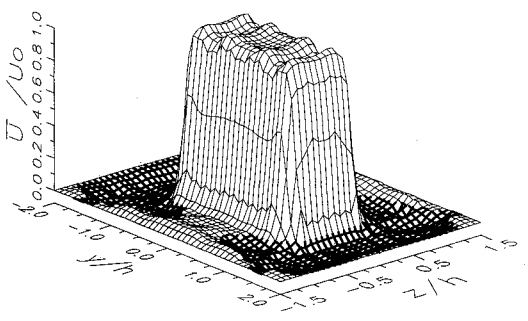

Fig. 9 $\bar{U}/U_0$ at $x/h = 0.5$. Negative flow is shown with heavy lines.

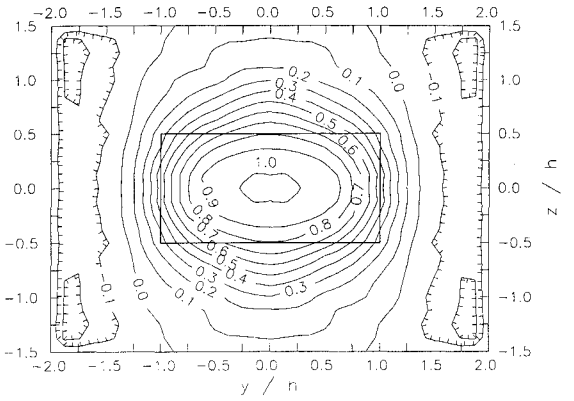

Fig. 10 $\bar{U}/U_0$ at $x/h = 3.0$.

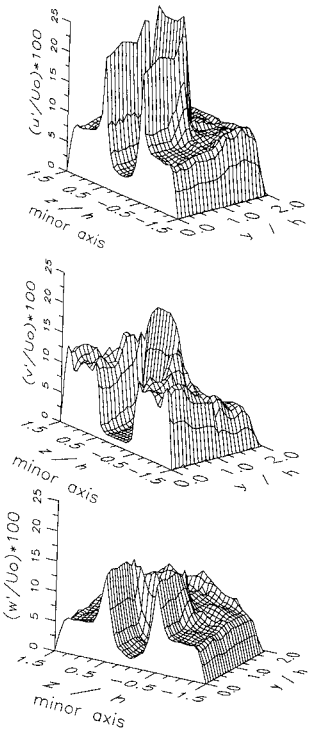

a)

b)

c)

Fig. 11 Velocity fluctuations at $x/h = 0.5$, percentage of U_0: a) u', b) v', and c) w'.

core of the jet has not switched axes. However, the shear layer on the minor axis has spread outward only, in accordance with the transverse velocity seen in Fig. 8b. This is in contrast to the shear layer on the major axis that has spread both inward and out. The outward spreading on the minor axis appears to be responsible for driving fluid into the outer corners, thus transferring fluid from the jet directly into the recirculation zone. This fluid moves back toward the step, where it is then transported back to the minor axis region and eventually entrained into the positive flow again.

A check on mass flow rate was made by assuming that the initial jet net mass flux is the integral of U_0 over the area of the upstream channel area, that is, by assuming plug flow. The net mass flux at $x/h = 0.5$, obtained by integrating $\bar{U}/U_0$ over the entire channel width using nonmirrored data, is low by 2% at $x/h = 0.5$ and is high by 8% at $x/h = 3$. When using nonmirrored data to the extent possible (three quadrants of the lower measurement plane were fully surveyed), the mass flow rate in the lower plane was high by 4%.

Figures 11a–11c show the normalized fluctuations for the three velocity components in the upper plane. In Fig. 11a, u'

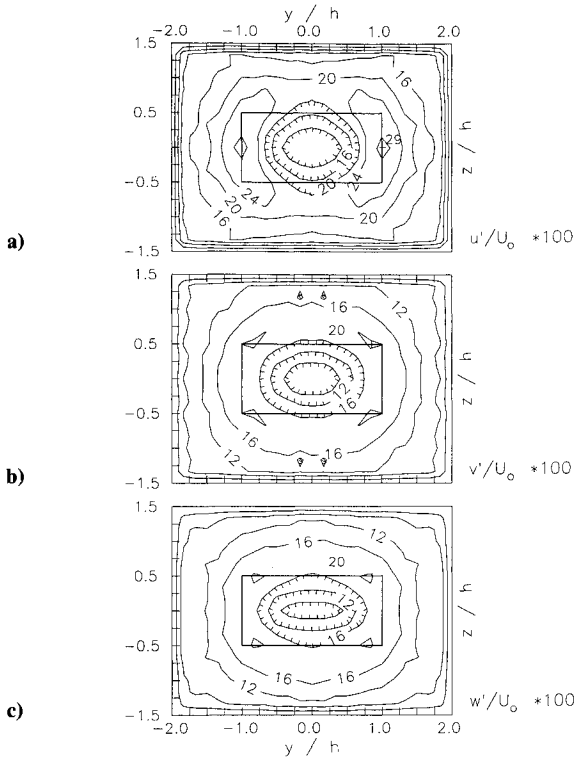

Fig. 12 Velocity fluctuations at $x/h = 3.0$, percentage of U_0: a) u', b) v', and c) w'.

forms a rectangular volcano shape. In the "caldera" of the volcano, the fluctuation level is quite low, 3%, equal to the incident turbulence plus the forcing perturbation. The axial fluctuations reach a maximum in the shear layer surrounding the core of the jet, resulting in the rim of the volcano. The outer region behind the step has a fairly uniform fluctuation level of 10%.

The transverse fluctuating components are not uniform around the jet. Figures 11b and 11c show that v' is much higher on the major than the minor axis, whereas w' is stronger on the minor. This is expected since the shear layer is still rectangular in cross section and the fluctuations normal to the layer will be higher than those "spanwise" to the layer. In addition to the peaks in the shear layer, there are other symmetric peaks near the walls in v' on the minor axis and in w' on the major. The v' peak can be explained by the fact that this region is at a stagnation point, where imbalances in the inflow from the sides can lead to high fluctuations. The reason for the peak in w' on the major axis is unclear, particularly since there is no mean W in region of the w' peak, nor any gradient in W that might lead to these fluctuations.

Figure 12 shows that farther downstream the transverse fluctuations are more uniform around the jet, and the peaks near the walls have disappeared. The axial fluctuations, seen in Fig. 12a, have developed maxima in the shear layer on the major axis. This may be related to the slightly steeper gradient in axial velocity on the major axis as compared with the gradient found on the minor axis. These axial velocity gradients can be seen in Figs. 5 and 10. Elliptic free jets also demonstrate this behavior.[1] There are also small peaks in v' and w' near the corners of the original jet. These may be related to the corners; in a study of free triangular jets, Schadow et al.[28] found higher turbulence downstream of the vertices.

Concluding Remarks

This flow provides an example of how a small deviation from a two-dimensionally symmetric flow can completely change the global features, revealing a new class of flow phenomena. For instance, in this rectangular sudden expansion the recirculation zone behind the backward-facing step is completely suppressed on the minor axis. This contrasts with the prediction from two-dimensional backward-facing step results, which indicate that for a flow with a higher expansion ratio, such as in the minor axis plane compared with the major axis plane, a longer recirculation zone should result.[14] Instead, no recirculation is found. In addition, significant transverse velocities are found that have no parallel in axisymmetric or plane-symmetric expansions.

These results may be due to the dynamics of the vortex structures in the shear layer surrounding the jet. Self-induction of the rectangular vortex ring would cause the jet to spread rapidly along the minor axis, as is seen in the time-averaged LDV results presented here. This spreading causes flow outward along the confining walls into the recirculation zone. When this fluid returns to the region behind the step, it is both entrained into the positive jet flow and carried into the minor axis region, where it is either entrained into the jet or turned into streamwise flow by the plane of symmetry.

Analysis of the ensemble-averaged data phase locked to the active forcing is expected to clarify these mechanisms.

Acknowledgments

This work was supported by a University Research Initiative contract from the U.S. Office of Naval Research and by the National Science Foundation. Our thanks to Mingdar (Gibson) Chen for his help with the figures.

References

[1]Ho, C. M., and Gutmark, E., "Vortex Induction and Mass Entrainment in a Small-Aspect-Ratio Elliptic Jet," *Journal of Fluid Mechanics,* Vol. 179, 1987, pp. 383–405.

[2]Kambe, T., and Takao, T., "Motion of Distorted Vortex Rings," *Journal of the Physical Society of Japan,* Vol. 31, No. 2, 1971, pp. 591–599.

[3]0shima, Y., "The Motion of Vortex Rings in Water," *Journal of the Physical Society of Japan,* Vol. 32, No. 4, 1972, pp. 1125–1131.

[4]Ho, C.M., and Huang, L.S., "Subharmonics and Vortex Merging in Mixing Layers," *Journal of Fluid Mechanics,* Vol. 119, 1982, pp. 443–473,

[5]Schadow, K. C., Wilson, K. J., and Gutmark, E., "Characterization of Large Scale Structures in Forced Ducted Flow with Dump," *AIAA Journal,* Vol. 25, No. 9, 1987, pp. 1164–1170.

[6]Bhattacharjee, S., Scheelke, B., and Troutt, T. R., "Modification of Vortex Interactions in a Reattaching Separated Flow," *AIAA Journal,* Vol. 24, No. 4, 1986, pp. 623–629.

[7]Roos, F. W., and Kegelman, J. T., "Control of Coherent Structures in Reattaching Laminar and Turbulent Shear Layers," *AIAA Journal,* Vol. 24, No. 12, 1986, pp. 1956–1963.

[8]Schadow, K. C., Gutmark, E., Wilson, K. V., and Parr, D. M., "Mixing Characteristics of a Ducted Elliptical Jet," *Journal of Propulsion and Power,* Vol. 4, No. 4, 1988, pp. 328–333.

[9]Schadow, K. C., Gutmark, E., Wilson, K. V., Parr, D. M., and Mahan, V. A., "Effect of Shear-Flow Dynamics in Combustion Processes," *Combustion Science and Technology,* Vol. 54, 1987, pp. 103–116.